Common mode noise modelling and resonant estimation in a three-phase motor drive system: 9-150 kHz frequency range

Rathnayake, Hansika; Ganjavi, Amir; Zare, Firuz; Kumar, Dinesh; Davari, Pooya

Published in:
2020 22nd European Conference on Power Electronics and Applications (EPE'20 ECCE Europe)

DOI (link to publication from Publisher):
10.23919/EPE20ECCEEurope43536.2020.9215887

Publication date:
2020

Document Version
Accepted author manuscript, peer reviewed version

Common-mode noise modelling and resonant estimation in a three-phase motor drive system: 9-150 kHz frequency range

Hansika Rathnayake[1], Amir Ganjavi[1], Firuz Zare[1], Dinesh Kumar[2], Pooya Davari[3],
[1] THE UNIVERSITY OF QUEENSLAND
St Lucia,
Brisbane, QLD 4072, Australia
E-Mail: h.rathnayake@uq.edu.au, f.zare@uq.edu.au, a.ganjavi@uq.net.au

[2] DANFOSS DRIVES A/S
6300 Gråsten, Denmark
E-Mail: dineshr30@ieee.org

[3] AALBORG UNIVERSITY
Aalborg, Denmark
E-Mail: pda@et.aau.dk

Acknowledgements

The authors would like to thank the Australian Research Council, supporting FT150100042 and LP170100902 projects.

Keywords

«common mode noise», «9-150 kHz harmonics», «three-phase motor drive », «resonance estimation», «EMI».

Abstract

This paper presents an equivalent circuit impedance-based estimation method of resonances in a three-phase motor drive system to predict common-mode (CM) noise circulations in 9-150 kHz frequency range, which is not considered so far in electromagnetic interference (EMI) analysis. The paper verifies the presented method by analyzing emission spectrums of CM currents in the three-phase system. The impact of EMI filter, DC-link filter and AC motor models on the generated common mode noise at 9-150 kHz range is also investigated using the predicted equivalent impedance results at the CM voltage source. It is found, there is a high probability to have resonances within 9-150 kHz range due to the components of the drive system. Hence, the work presented is useful to model and predict the possible resonances in the whole drive system that unnecessarily increases the CM noise at this frequency range. The presented estimation method not only enables the ability to early recognition of CM current emissions injected from the drive system to the grid but also supports EMI filter design or modification for 9-150 kHz frequency range. Further, this approach significantly contributes to accelerating the drive products development and entering the market after complying the future standards.

Introduction

The increasing trend of high-frequency switching inverters (in kHz range) in adjustable speed drives cause increasing the noise emissions beyond 2 kHz which are above the traditional frequency range. This introducing, new high-frequency emissions lie between 2-150 kHz frequency range resulting in critical and widespread power quality issues in the near future. As reported, sensitive equipment damage, low power quality and stability issues in distribution networks can happen due to the unregulated disturbance level emission from the noise sources within this new frequency range [1]-[6].

Inverters in three-phase motor drive systems utilize low or high switching frequency depending on the power level. The high voltage slew rates (dv/dt) across the inverters due to this switching operation causes Electromagnetic interference (EMI) noises [7]. The EMI emission with differential mode (DM) and CM noise critically affect the function of electrical and electronic devices connected to the point of common coupling. Although these noises are well defined for single-phase systems, there is a limited research work for three-phase systems such as three-phase adjustable speed drives. However, in three-phase systems, CM noise can be defined as "ground -included-loop noise" and DM noise can be defined as "line-to-line noise" [8]. IEC /CISPR standards are generally defined the EMI noises from 150 kHz to 30 MHz for distribution networks. Besides, Line Impedance Stabilization Network (LISN) recommended by CISPR16 standards are used for EMI measurement in the range of 9 kHz- 30 MHz to maintain fixed impedance at the grid point and to decouple high frequency between the mains and the drive system. As the standards and measurement methods for 2-150 kHz frequency range have not been completed to cover all products including adjustable motor drives, IEC Technical Committee 77A is currently working on this new standardization process [5]. According to this team activity, the frequency range has been split into two main frequency bands as 2-9 kHz and 9-150 kHz. Discussions on upcoming standards are presented in [9, 10]. In parallel to a standardisation activity, recent studies on 2-150 kHz frequency range have been presented in [10]-[18]. These works focus on harmonic modelling of multi-parallel grid-tied inverters [11, 12] and different inverter topologies [13]-[15], [18], grid impedance estimation [16] and harmonic measurement techniques [10, 17] within this new frequency range. However, the contribution of EMI filters and DC-link filters in the motor drive systems towards the 2-9 kHz and 9-150 kHz harmonics have not been addressed in the literature.

The equivalent circuit-based EMI analysis of three-phase PWM rectifier of 1 MHz [19] and 100 kHz [20] switching frequencies are presented. In [21], an impedance equivalent circuit based EMI filter design procedure is demonstrated for a diode rectifier connected inverter motor drive system operating at 15 kHz switching frequency. However, the effect of practical models of components in the high-frequency range has not been considered for their design or analysis. Even though, reference [22] demonstrates the effect of parasitic parameters on a generic EMI filter of AC/DC converters, the system modelling and resonance analysis with the filter for a particular application are not covered. Moreover, all the above literature have presented their work for 150 kHz- 30 MHz frequency range to comply with the existing EMI standards. Therefore, it is essential to analyze the 9-150 kHz harmonic behaviour of three-phase motor drive systems with the existing EMI and DC-link filters together with the AC motor. Considering this research gap, a systematic study is timely valued for motor drive manufacturers to design a cost-effective filter to suppress emissions within this new frequency range. Therefore, this paper presents a method to model and estimate resonances causing CM noise increase in overall three-phase motor drive system within 9-150 kHz frequency range to analysis and design EMI filter considering the upcoming future standard requirement.

This paper presents equivalent circuit-based modelling and estimation method of resonances of the three-phase motor drive system to predict the level of CM noise circulations in the system. The method is further verified by the frequency response analysis of CM currents in the three-phase system. Impact of EMI filter, DC-link filter, and AC motor nonlinear frequency characteristics to the CM noise is also comprehensively demonstrated using the equivalent impedance results at the CM voltage source. Generally, the resonances created by the inductor, capacitor elements of the overall motor drive systems including filters cannot be seen beyond 150 kHz, so that there is no effect from resonances when complying the existing EMI standards. In contrast, as found, there is a high probability to have those resonances within 9-150 kHz range. Hence, the work presented is useful to model and predict the possible resonances in the whole drive system that unnecessarily increases the CM noise at this new frequency range. The presented estimation method not only enables the ability to early recognition of CM current emissions injected from the drive system to the grid but also supports EMI filter design/modification for 9-150 kHz frequency range. Thus, this paper significantly contributes to accelerating the drive products development and entering the market with possible compliance of upcoming EMI standards for 9-150 kHz frequency range.

System Description

The motor drive system generally consists of a rectifier, DC-link, inverter and AC motor. Besides, there is a DC filter and EMI filter in the drive system to comply with the existing low frequency (0-2 kHz) and EMI (150 kHz- 30 MHz) standards, respectively. Fig. 1 shows the overall structure of the studied three-phase PWM inverter motor drive system. The low impedance, CM noise propagation paths in the high-frequency range are created due to the capacitive couplings between the AC motor and the ground. To avoid these CM currents flowing to the grid, typically filter designers introduce low impedance path of EMI filter capacitors (Cy_{AC}) to the ground and the DC-link mid-point capacitor (Cy_{DC}) to ground. Thus, for the topology given in Fig.1, there are four main CM currents in the total system generated by the Pulse Width Modulated voltage. These CM currents are through the motor ($i_{g\text{-}motor}$), DC-link capacitor ($i_{g\text{-}dc\text{-}link\ cap}$), EMI filter ($i_{g\text{-}EMI\ filter}$) and grid ($i_{g\text{-}grid}$) as shown in Fig.1. In this paper, the effect of cable is not considered assuming there is a short cable in between the inverter and the motor. Moreover, the effect of capacitive couplings of heatsink can be neglected in this study due to its low capacitance below 150 kHz.

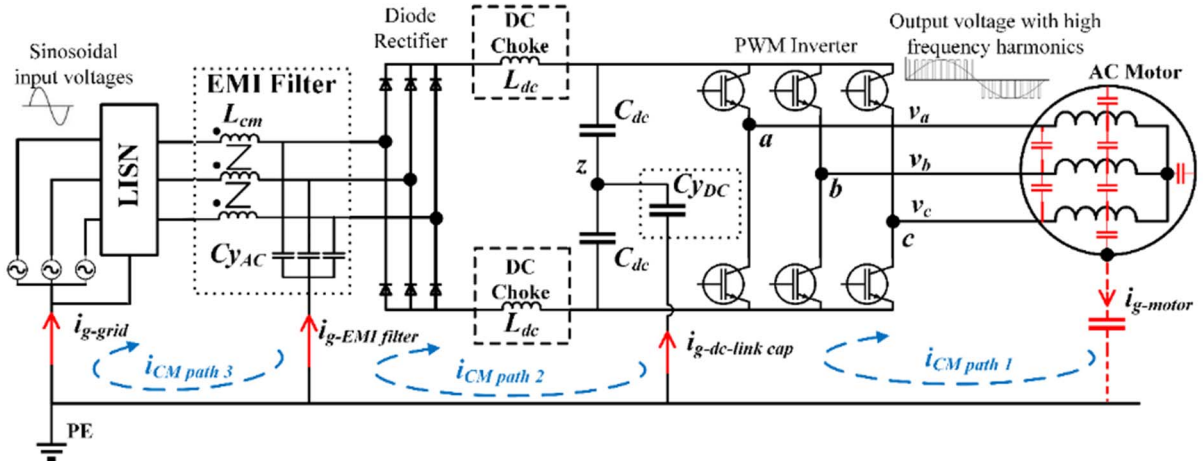

Fig. 1: Overall structure of the studied three-phase PWM inverter motor drive system for CM analysis

Modelling and resonant estimation of common-mode loop at 9-150 kHz

The three-phase system is simplified to an equivalent single-phase circuit for the CM noise analysis based on the fact "ground -included-loop noise" of the system and parallel concept of all phases with CM noise propagation. The CM voltage of inverter with respect to mid-point of the DC-link "*z*" represents the CM noise source due to the PWM with a high switching frequency (kHz to MHz range) of the inverter. When the system operates using double-edge naturally sampled PWM, the analytical harmonic solutions for phase voltages ($v_{i\,z}$ where i=a, b, c) of the inverter output concerning z can be expressed as (1) [23]. Here, the V_{dc} is one-half of DC-link voltage. Then the CM voltage (v_{com}) generated by PWM at the inverter terminal can be derived as (2). From (1) and (2), the harmonics of v_{com} (v_{com_h}) can be derived as (3), in which the harmonic occurrence depends on the multiples of the carrier/switching frequency and the fundamental frequency. In order to represent the high-frequency behaviour of the system in Fig. 1, practical models of EMI filter, DC-choke, DC-link capacitor and AC motor are derived. It should be noted that all these practical models are developed based on the experimental measurements of each component using a network analyzer (Bode 100). The system specifications are tabulated in Table I. With the high-frequency noise source- v_{com} and practical models of each component, the derived CM equivalent circuit for the studied system in Fig. 1 is shown in Fig. 2. This paper uses the CISPR16 LISN [2] which is still utilized in the industry in the 9- 150 kHz range analysis since this is the only available in the EMI/EMC measurement standards. Thus, to estimate the CM resonances at 9-150 kHz frequency range, the equivalent impedance of the system (Z_T) seen from the CM noise source is evaluated, as shown in Fig. 2.

$$v_{iz}(t) = V_{dc}M\cos(\omega_o t+\theta_i)+\frac{4V_{dc}}{\pi}\sum_{m=1}^{\infty}\sum_{n=-\infty}^{\infty}\frac{1}{m}J_n(m\frac{\pi}{2}M)\sin([m+n]\frac{\pi}{2})\cos(m\omega_c t+n[\omega_o t+\theta_i]) \quad (1)$$

Where M = modulation index, m, n = carrier, baseband index variable, ω_c, ω_o = angular frequency of carrier waveform, fundamental voltage, $J_n(x)$ = Bessel function of order n and argument $x = m\frac{\pi}{2}M$, $\theta_{i=a,b,c} = 0, -\frac{2\pi}{3}, \frac{2\pi}{3}$

$$v_{com}(t) = \frac{v_{az} + v_{bz} + v_{cz}}{3} \tag{2}$$

$$v_{com\_h}(t) = \frac{4V_{dc}}{3\pi}\sum_{m=1}^{\infty}\sum_{\substack{n=-\infty \\ n\neq 0}}^{\infty}\frac{1}{m}J_n(m\frac{\pi}{2}M)\sin([m+n]\frac{\pi}{2})\{1+2\cos(n\frac{2\pi}{3})\}\cos(m\omega_c t + n\omega_o t) \tag{3}$$

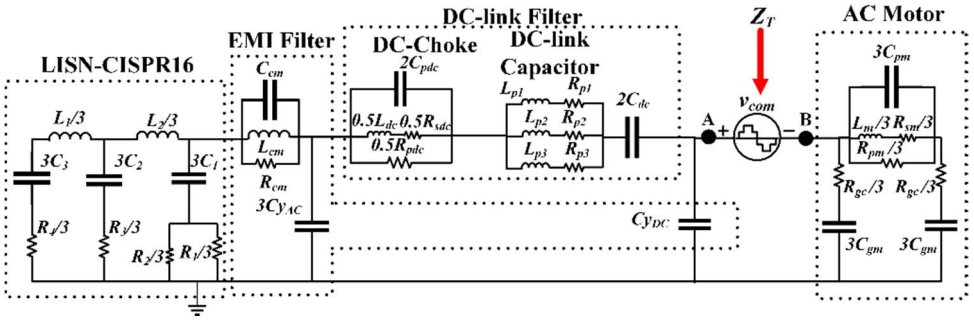

Fig. 2: Equivalent CM circuit of three-phase motor drive system to estimate resonances at 9-150 kHz

Table I: Specifications of the drive system

Filters	Value	Motor Drive	Value
L_{dc}, R_{sdc}, R_{pdc}	1.25 mH, 0.28 Ω, 1.29 kΩ	L_m	9.4 mH
C_{dc}, C_{pdc}	1000 µF, 228 pF	C_{pm}	4.5 pF
L_{p1}, L_{p2}, L_{p3}	0.37 µH, 15.28 µH, 21.3 µH	C_{gm}	1100 pF
R_{p1}, R_{p2}, R_{p3}	0.27 Ω, 0.57 Ω, 1.13 Ω	R_{sm}, R_{pm}	9.5 Ω, 12.7 kΩ
C_{cm}, R_{cm}	88 pF, 0.5 MΩ	f_o, f_c, Power rating	50 Hz, 5 kHz, 7.5 kW

Sensitivity analysis of system parameters to the resonances at 9-150 kHz

According to the proposed resonance estimation approach using Z_T, sensitivity analysis of system parameters towards the resonances at 9-150 kHz is presented in this section. Namely, the effect of damping of AC motor, practical filter components of DC-link and EMI filter and different motor types are comparatively demonstrated.

Case 1: A system model with ideal filter components and a high-frequency model of AC motor without damping effect

If EMI filter and DC-link filter are ideal, only inductor values, L_{cm} and L_{dc} are in the system. Therefore, the high frequency (HF) behaviour of components of L_{cm} and L_{dc} are not included in the ideal condition of the system in this case 1. Moreover, the HF model of AC motor without damping effect (without damping R=R_{sm}, R_{pm}, R_{gc} in each phase) is also considered to present this ideal system. Then the Z_T is analyzed for the system with these ideal filter components and undamped AC motor. As shown in Fig. 3, there are two severe resonances in the system at 20 kHz and 50 kHz, which create very low impedances to increase the i_{CM} current harmonics when harmonics of v_{com} occur at those frequencies.

This type of resonances is not acceptable in a real system due to the possible, unprotective, high level of leakage current flow through the system.

Case 2: Damping effect of AC motor

In case 2, the effect of damping R (R_{sm}, R_{pm}, R_{gc} in each phase) of the AC motor to the identified resonances is presented. It should be noted that the filters are in ideal condition with only L_{cm} and L_{dc} as in case 1. Fig. 4 shows the Z_T when the AC motor has a damping R according to its static HF model. The results show that there is a significant effect for the damping of the resonance at 50 kHz due to high-frequency model of the AC motor and its damping effect. In addition, it is verified that generally this high-end resonance (50 kHz) of 9-150 kHz range is created by the AC motor, even though there are other magnetic elements in the system. It is also revealed the importance of an accurate model of AC motor in the CM noise studies of 9-150 kHz frequency range.

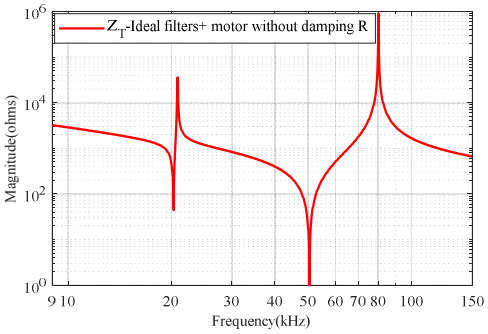

Fig. 3: Case 1- Equivalent impedance (Z_T) for the ideal system

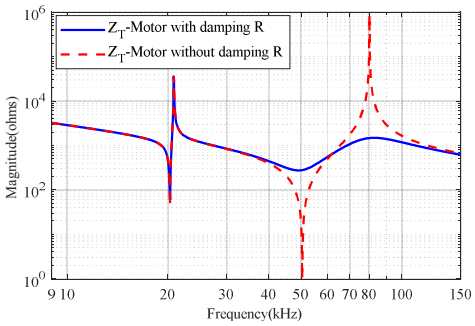

Fig. 4: Case 2- Z_T for Case 1 and system including AC motor with damping R

Case 3: Practical effects of filter components

The HF models of the EMI filter consists of damping resistor (R) of R_{cm} and parasitic capacitive couplings of C_{cm}. Similarly, DC-link filter consists of damping R of R_{sdc} and R_{pdc} together with the parasitic capacitor of C_{pdc} as shown in Fig. 2. According to Z_T shown in Fig. 5 (a), it is found that the filter damping R has a promising impact on the damping of resonance at 20 kHz. However, capacitive couplings of filter inductors do not affect system resonances as seen in Fig. 5(b).

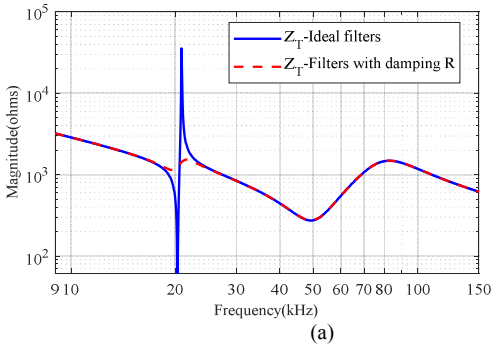

(a)

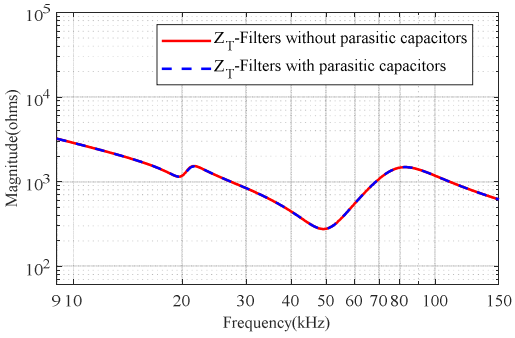

(b)

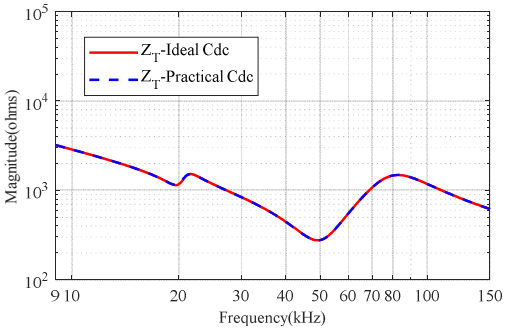

(c)

Fig. 5: Case 3- Z_T with practical filter components (a) Case 2 and system with filter damping R (b) with filter damping R and parasitic capacitors (c) with ideal and practical DC-ink capacitor (C_{dc}) model

The DC-link Electrolytic capacitor has an inductive behaviour at high frequencies introducing an HF model to the ideal C_{dc} in practice. Each DC-choke is in series with each DC-link capacitor, C_{dc} as per the CM loop current flow due to the DC-link mid-point grounded capacitor Cy_{DC}. This can be seen in the equivalent circuit shown in Fig. 2. As a result, the DC-choke is dominant for the resonance at 20 kHz in the CM loop. Therefore, there is no effect from the practical DC-link capacitor to the CM impedance, as seen in Fig. 5(c).

Case 4: Impacts of different motor types (grounding capacitive coupling)

It is well-known that selecting an AC motor with a very low grounding capacitive couplings (C_{gm}) is a perfect solution for reducing CM current flow in the three-phase motor drive systems. However, according to the application and other factors, optimizing the AC motor by the customer is not feasible. Even though selecting a motor is not a concern of the drive manufacturers, the EMI compatible drives must be designed by considering the worst cases of the possible motor systems. Therefore, it is essential to study the impact of different motors (i.e., different C_{gm}) towards the Z_T to understand its level of contribution on i_{CM}. As seen in Fig. 6, higher C_{gm} (200% of C_{gm}) of AC motors shifts the resonances of both 20 kHz and 50 kHz to lower frequencies (to 19 kHz and 35 kHz), while reducing the level of overall impedance that can affect for rising the overall CM current harmonic levels including at these two resonances. However, Z_T between 40 kHz to 70 kHz has been increased with the higher capacitive coupling, making the system less sensitive to v_{com} harmonics at this range.

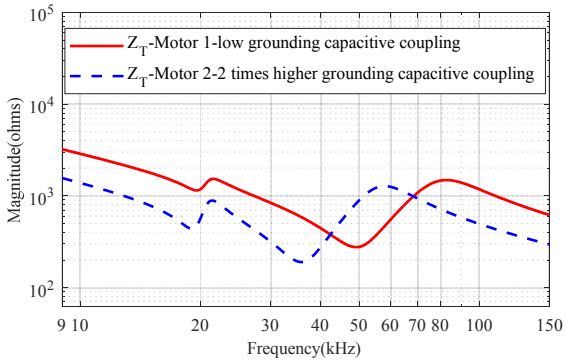

Fig. 6: Case 4- Z_T for the system with AC motors of different grounding capacitive couplings

Case 5: Impacts of DC link filter parameters L_{dc} and C_{dc}

The main components of the DC link filter are L_{dc} and C_{dc}. Fig. 7(a) and Fig. 7(b) show the effect of these filter parameters. There is a high probability of saturation of DC choke at high frequencies, causing the drop of L_{dc}. If L_{dc} drops to 50% of its value, there is a definite shift of 20 kHz resonance towards 29 kHz that can be seen in Fig. 7(a). However, there is no effect for Z_T or resonances at the frequency range of 9-150 kHz by 50% decrease of C_{dc} (See Fig. 7(b)). From the results of Fig. 5(a) and Fig. 7(a), it is further confirmed this low-end resonance of 9-150 kHz range is mainly due to the DC choke.

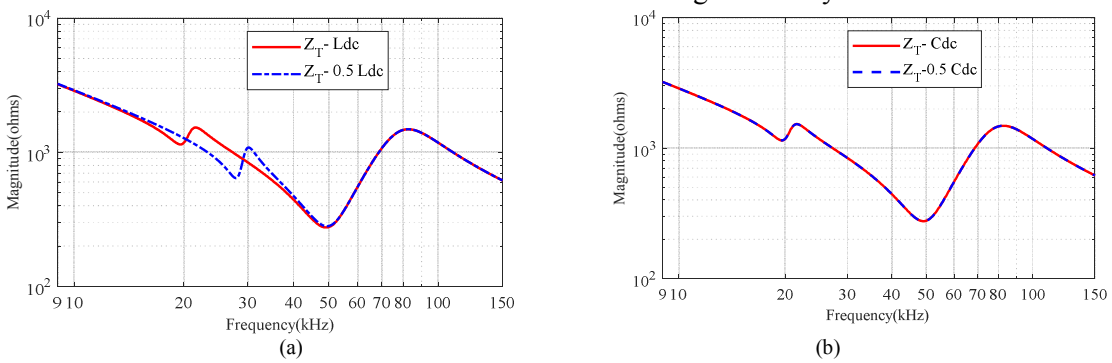

Fig. 7: Case 5- Z_T with different DC- link filter parameters (a) different L_{dc} (b) different C_{dc}

Case 6: Impacts of EMI filter parameters

The main components of the EMI filter can be listed as CM choke inductance (L_{cm}), Cy_{AC} and Cy_{DC}. When analyzing the effect of these EMI filter parameters, it is found that 50% decrease of L_{cm} representing the saturation of CM choke, shows no effect for 9-150 kHz range resonances as shown in

Fig. 8(a). The 50% decrease of grounding capacitor, Cy_{AC} introduces a slight shift of the 20 kHz resonance that is negligible as depicted in Fig. 8(b). In contrast, the 50% decrease of grounding capacitor, Cy_{DC} has significantly shifted the first resonance of this frequency range from 20 kHz to 27 kHz, as shown in Fig. 8(c). It is also revealed that the value of Cy_{DC} plays a significant contribution to the low-end resonance of 9-150 kHz range (20 kHz) together with the value of L_{dc} (See Fig. 7(a)) compared to other filter parameters.

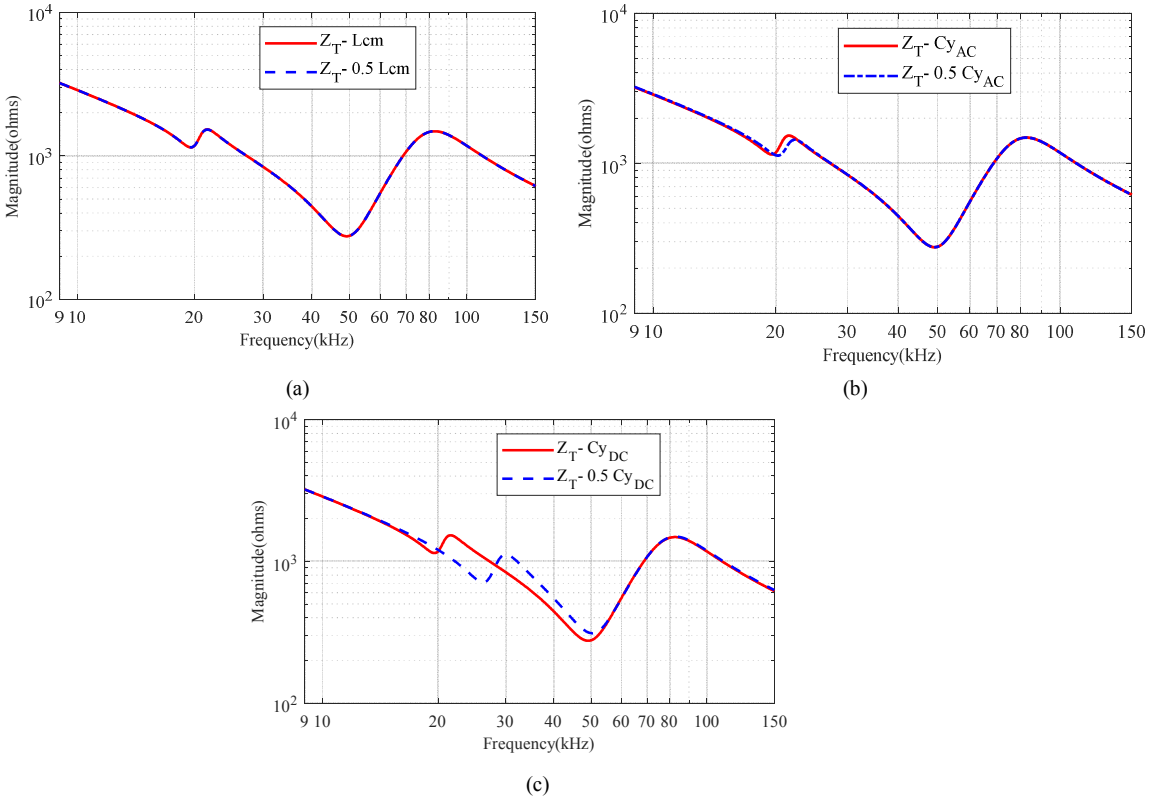

Fig 8: Case 6- Z_T with EMI filter parameters (a) different L_{cm} (b) different Cy_{AC} (c) different Cy_{DC}

Verification of the resonance estimation method using common-mode noise loops of the three-phase motor drive system

In order to verify the equivalent circuit-based impedance analysis for estimation of possible resonances affecting the CM noise, frequency response (FFT) of i_{CM} currents ($i_{g\text{-}motor}$, $i_{g\text{-}dc\text{-}link\ cap}$, $i_{g\text{-}EMI\ filter}$ and $i_{g\text{-}grid}$) of the three-phase system shown in Fig. 1 are analyzed in the Matlab/Simulink simulation platform. The impact of PWM strategy to the CM noise is not the scope for this study so that SPWM with 5 kHz switching frequency is used for the overall study.

The results for case 1 are shown in Fig. 9 (a). The identified resonances for the system using Z_T in the previous section are 20 kHz and 50 kHz. The significant resonance at 50 kHz mainly can be seen in $i_{g\text{-}motor}$ and $i_{g\text{-}dc\text{-}link\ cap}$, where $i_{g\text{-}EMI\ filter}$ and $i_{g\text{-}grid}$ also have 300 mA and 0.5 mA of 50 kHz noise. The resonance at 20 kHz also can be seen in $i_{g\text{-}dc\text{-}link\ cap}$ and $i_{g\text{-}EMI\ filter}$ of around 50 mA while $i_{g\text{-}grid}$ has 0.5 mA of its magnitude. These results validate the resonance estimation method using Z_T in Fig. 3. Each resonance circulates through different loops in different ratios depends on the impedance ratio at different frequency instants. However, as expected, $i_{g\text{-}grid}$ has a lower magnitude noise (0.5 mA) at these critical resonances compared to other i_{CM} currents shown due to the internal DC-side and AC-side filtering paths. Further, FFT results of i_{CM}s for case 3 (b) are shown in Fig. 9 (b). The results clearly show the reduced magnitudes of each i_{CM} at above resonances due to the damping R and capacitive couplings of filters and AC motor. In this case, $i_{g\text{-}grid}$ is less than 0.5 mA at 20 kHz and less than 0.1 mA at 50 kHz. The Z_T result in Fig. 5(b) also shows this damping of resonances.

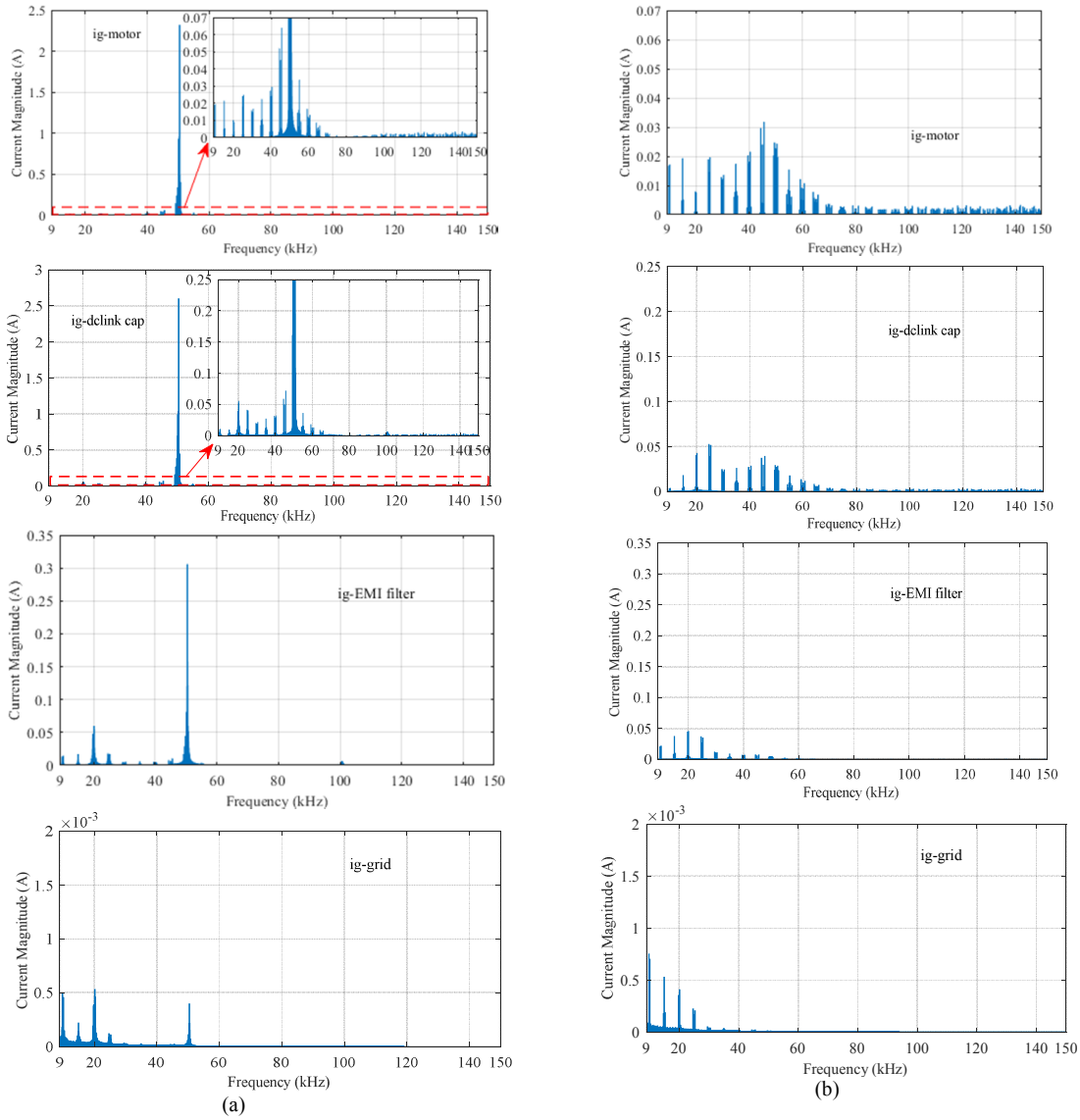

Fig 9: FFT of i_{CM}s in Fig. 1 (a) Case 1 (b) Case 3(b)

The effect of increased grounding capacitive coupling of the AC motor is presented in case 4. FFT results of i_{CM}s for case 4 are shown in Fig. 10 (a). The results clearly show the increased magnitudes of all i_{CM} currents compared to Fig. 9(b). This can be comparable with Z_T result in Fig. 6, which shows lower impedance values with increased capacitive couplings to cause high i_{CM}. The estimated shift of the most critical high-end resonance to 35 kHz is also can be clearly seen in $i_{g\text{-}motor}$, $i_{g\text{-}dc\text{-}link\ cap}$, and $i_{g\text{-}EMI\ filter}$. Comparing Fig. 9(b) and Fig. 10(a), it highlights even though the same filtering system is available,the noise of $i_{g\text{-}grid}$ at 9-150 kHz can increase due to the poorly designed AC motors with high grounding couplings.

The frequency response of i_{CM}s for case 5(a) are shown in Fig. 10 (b). The effect of L_{dc} saturation is presented in this case. According to Z_T result in Fig. 7(a), a resonance shit is estimated. This estimated shift of the low-end resonance to 29 kHz is also can be clearly seen in $i_{g\text{-}dc\text{-}link\ cap}$, $i_{g\text{-}EMI\ filter}$ and $i_{g\text{-}grid}$. Comparing the typical case in Fig. 9(b), $i_{g\text{-}grid}$ of Fig. 10(b) has been increased at 29 kHz, reflecting the resonance shift of Z_T and magnitude drop of Z_T at this new resonance with the L_{dc} saturation.

Thus, it is verified the estimated resonances in the three-phase system are comparable with the proposed Z_T analysis. Moreover, the results clearly show that the $i_{g\text{-}grid}$ significantly reduces as expected, due to the internal i_{CM} current flow paths created by the DC-filter and EMI filter.

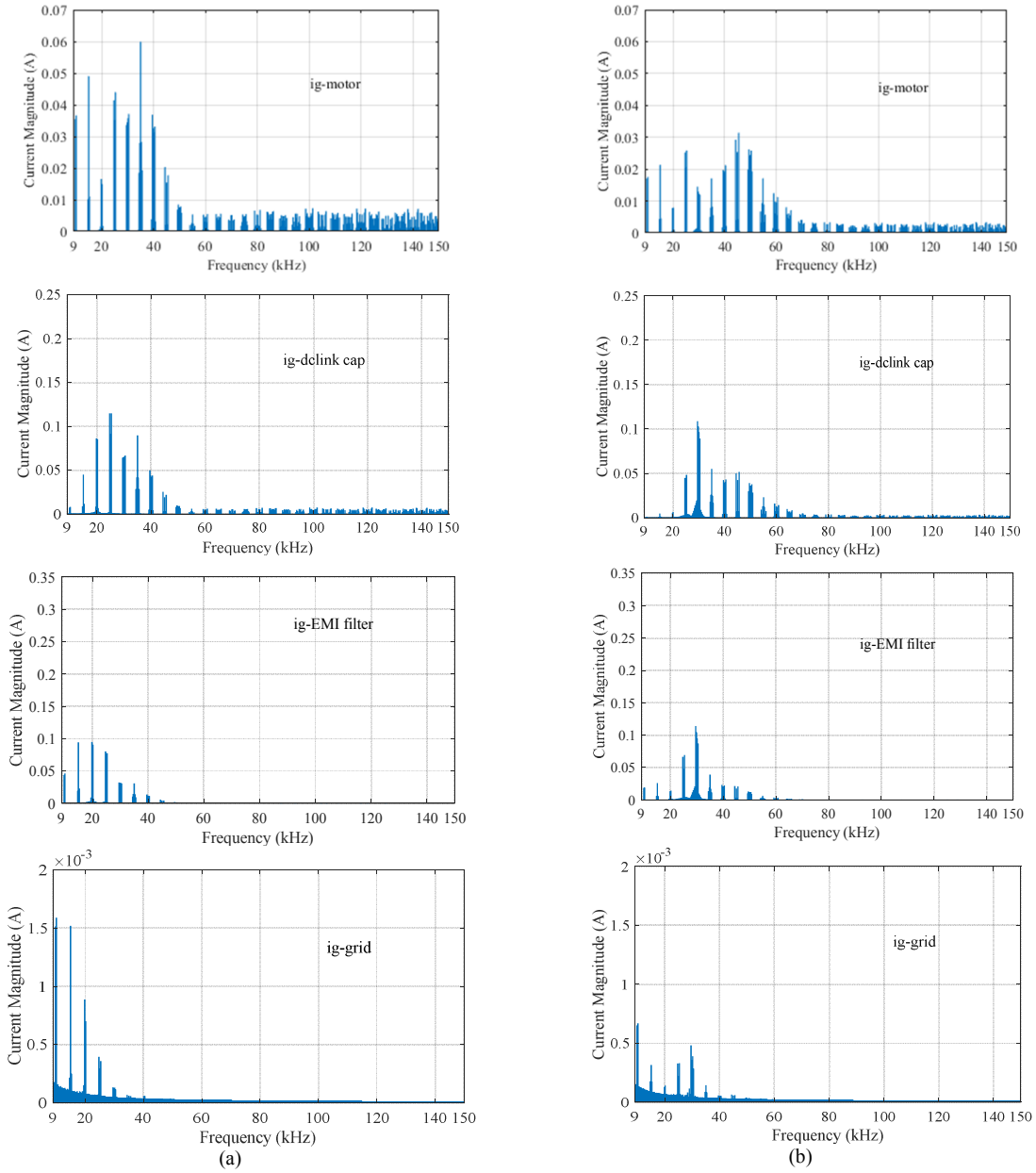

Fig 10: FFT of i_{CM}s in Fig. 1 (a) Case 4 (b) Case 5(a)

Conclusions

This paper presents and verifies an equivalent CM impedance analysis method for three-phase motor drive systems to identify the possible resonances in the frequency range of 9-150 kHz, addressing future standards. It is found that there are resonances in this frequency range that can be effectively damped using the damping resistors of both filters' and AC motor's high-frequency models. It is found that effect from a practical model of DC-link capacitor to the CM loop is negligible since the DC-choke inductance plays the dominant role in the resonance of CM noise. AC motor grounding capacitive couplings shift the locations of all resonance frequencies, especially the high-end resonance of 9-150 kHz range while changing CM impedance at the noise source. In contrast, DC-choke and DC-side grounding capacitor of EMI filter only affect the low-end resonance of this frequency range. Thus, investigation of practical models of components in the overall system when designing EMI and DC-link filters is essential to exploit the system damping effect at resonance frequencies in 9-150 kHz and to achieve the expected performance for CM noise effectively. Further, the presented work is a benchmark for the EMI filter design, when complying with the upcoming EMI standards of 9-150 kHz frequency range.

References

[1] D. Fallows, S. Nuzzo, A. Costabeber, and M. Galea, "Harmonic reduction methods for electrical generation: a review," *IET Generation, Transmission & Distribution,* vol. 12, no. 13, pp. 3107-3113, 2018.

[2] P. Davari, F. Blaabjerg, E. Hoene, and F. Zare, "Improving 9-150 kHz EMI Performance of Single-Phase PFC Rectifier," in *CIPS 2018; 10th International Conference on Integrated Power Electronics Systems*, 2018, pp. 1-6.

[3] D. Kumar and F. Zare, "Harmonic Analysis of Grid Connected Power Electronic Systems in Low Voltage Distribution Networks," *IEEE Journal of Emerging and Selected Topics in Power Electronics,* vol. 4, no. 1, pp. 70-79, 2016.

[4] J. Yaghoobi, A. Abdullah, D. Kumar, F. Zare, and H. Soltani, "Power Quality Issues of Distorted and Weak Distribution Networks in Mining Industry: A Review," *IEEE Access,* vol. 7, pp. 162500-162518, 2019.

[5] F. Zare, H. Soltani, D. Kumar, P. Davari, H. A. M. Delpino, and F. Blaabjerg, "Harmonic Emissions of Three-Phase Diode Rectifiers in Distribution Networks," *IEEE Access,* vol. 5, pp. 2819-2833, 2017.

[6] J. Yaghoobi, A. Alduraibi, D. Martin, F. Zare, D. Eghbal, and R. Memisevic, "Impact of high-frequency harmonics (0–9 kHz) generated by grid-connected inverters on distribution transformers," *International Journal of Electrical Power & Energy Systems,* vol. 122, p. 106177, 2020.

[7] F. Zare, (2009) "EMI Issues in Modern Power Electronic Systems", *The IEEE EMC Society Newsletters*, pp. 53-58.

[8] A. Kempski and R. Smolenski, "Decomposition of EMI Noise into Common and Differential Modes in PWM Inverter Drive System," *Journal of Electrical Power Quality and Utilisation,* vol. 12, no. 1, 2006.

[9] M. Bollen, M. Olofsson, A. Larsson, S. Rönnberg, and M. Lundmark, "Standards for supraharmonics (2 to 150 kHz)," *IEEE Electromagnetic Compatibility Magazine,* vol. 3, no. 1, pp. 114-119, 2014.

[10] J. Meyer *et al.*, "Future work on harmonics - some expert opinions Part II - supraharmonics, standards and measurements," in *2014 16th International Conference on Harmonics and Quality of Power (ICHQP)*, 2014, pp. 909-913.

[11] K. G. Khajeh, D. Solatialkaran, F. Zare, and N. Mithulananthan, "Harmonic Analysis of Multi-Parallel Grid-Connected Inverters in Distribution Networks: Emission and Immunity Issues in the Frequency Range of 0-150 kHz," *IEEE Access,* vol. 8, pp. 56379-56402, 2020.

[12] M. Klatt, R. Stiegler, J. Meyer, P. J. I. G. Schegner, Transmission, and Distribution, "Generic frequency-domain model for the emission of PWM-based power converters in the frequency range from 2 to 150 kHz," *IET Generation, Transmission & Distribution,* vol. 13, no. 24, pp. 5478-5486, 2019.

[13] D. Darmawardana *et al.*, "Investigation of high frequency emissions (supraharmonics) from small, grid-tied, photovoltaic inverters of different topologies," in *2018 IEEE 18th International Conference on Harmonics and Quality of Power (ICHQP)*, 2018, pp. 1-6.

[14] H. Rathnayake, D. Solatialkaran, F. Zare, and R. Sharma, "Grid-tied Inverters in Renewable Energy Systems: Harmonic Emission in 2 to 9 kHz Frequency Range," in *2019 21st European Conference on Power Electronics and Applications (EPE '19 ECCE Europe)*, 2019, pp. 1- 10.

[15] H. Rathnayake, K. G. Khajeh, F. Zare, and R. Sharma, "Harmonic Analysis of Grid-tied Active Front End Inverters for the Frequency Range of 0 - 9 kHz in Distribution Networks:Addressing Future Regulations," in *2019 IEEE International Conference on Industrial Technology (ICIT)*, 2019, pp. 446-451.

[16] M. M. A. Nezhadi, H. Hassanpour, and F. Zare, "A New High Frequency Grid Impedance Estimation Technique for the Frequency Range of 2 to150 kHz," *International Journal of Engineering* vol. 31, no. 10, pp. 1666-1674, 2018.

[17] I. Angulo, A. Arrinda, I. Fernández, N. Uribe-Pérez, I. Arechalde, and L. Hernández, "A review on measurement techniques for non-intentional emissions above 2 kHz," in *2016 IEEE International Energy Conference (ENERGYCON)*, 2016, pp. 1-5.

[18] K.G. Khajeh, D. Solatialkaran, F. Zare, and M. Nadarajah, "Harmonic Analysis of Grid-connected Inverters Considering External Distortions: Addressing Harmonic emissions up to 9kHz," *IET Power Electronics,* 2020.

[19] M. Hartmann, H. Ertl, and J. W. Kolar, "EMI Filter Design for a 1 MHz, 10 kW Three-Phase/Level PWM Rectifier," *IEEE Transactions on Power Electronics,* vol. 26, no. 4, pp. 1192-1204, 2011.

[20] A. Mallik, W. Ding, and A. Khaligh, "A Comprehensive Design Approach to an EMI Filter for a 6-kW Three-Phase Boost Power Factor Correction Rectifier in Avionics Vehicular Systems," *IEEE Transactions on Vehicular Technology,* vol. 66, no. 4, pp. 2942-2951, 2017.

[21] P. Chen and Y. Lai, "Effective EMI Filter Design Method for Three-Phase Inverter Based Upon Software Noise Separation," *IEEE Transactions on Power Electronics,* vol. 25, no. 11, pp. 2797-2806, 2010.

[22] W. Shuo, F. C. Lee, D. Y. Chen, and W. G. Odendaal, "Effects of parasitic parameters on EMI filter performance," *IEEE Transactions on Power Electronics,* vol. 19, no. 3, pp. 869-877, 2004.

[23] D. G. Holmes and T. A. Lipo, *Pulse Width Modulation for Power Converters: Principles and Practice*. Wiley-IEEE Press, 2003.